Physics-Aided RUL Prediction of Pick-and-Place Robotic Arm Using Dynamic Simulation and GMM-Based Health Indicator

Mujin Kim, Sejun Park, Heoung-Jae Chun and Jongsoo Lee*

*School of Mechanical Engineering, Yonsei University, Seodaemun-gu, Seoul, 03722, Korea

jini7017@yonsei.ac.kr
sejoon1227@yonsei.ac.kr
hjchun@yonsei.ac.kr
jleej@yonsei.ac.kr

ABSTRACT

Pick-and-place robotic arms driven by closed-loop servo motors operate under repetitive trapezoidal motion profiles (acceleration–constant speed–deceleration–stop), which yield non-stationary and multi-modal signal distributions and can undermine conventional distance-based anomaly detection and health indicators. This paper proposes a physics-aided prognostics and health management (PHM) framework for a one-degree-of-freedom servo-driven robotic joint. Based on failure mode and effects analysis (FMEA), bearing degradation (represented as increased friction torque) and shaft misalignment (represented as an eccentric disturbance torque) are selected as critical degradation mechanisms. To address the scarcity of industrial run-to-failure data, a high-fidelity Modelica dynamic model of a motor–shaft/bearing–compliance–load drivetrain is developed to synthesize progressive degradation scenarios. We first show that principal component analysis (PCA) visualization and a Mahalanobis-distance-based indicator can be unreliable because healthy data form multiple clusters induced by the servo operating phases. To explicitly capture healthy multi-modality, we train a Gaussian mixture model (GMM) using healthy modes and define a probabilistic health indicator as the negative log-likelihood (NLL) under the learned healthy distribution; the indicator shows an increasing trend across the designed degradation scenarios with degradation progression. The health indicator is then normalized between healthy and failure thresholds to construct a normalized remaining useful life (Normalized-RUL) index that provides a relative life measure without requiring ground-truth failure-time labels. Finally, continuous Normalized-RUL trajectories are estimated using a continuous wavelet transform–long short-term memory (CWT–LSTM) model that learns time–frequency degradation patterns and their temporal evolution. In the most severe simulated condition, the predicted remaining life decreases to approximately 40% of the nominal life, demonstrating the potential of the proposed framework for predictive maintenance of servo-driven robot joints.

1. Introduction

Pick-and-place robotic arms are indispensable assets in smart manufacturing, where unplanned downtime directly reduces throughput and increases maintenance cost. Servo-driven joints and reducers undergo repetitive, high-cycle motion and frequent acceleration–deceleration stresses, which can gradually degrade transmission elements and compromise positioning accuracy. Accordingly, prognostics and health management (PHM) for industrial robot joints has attracted increasing interest, spanning both condition monitoring for early fault detection and remaining useful life (RUL) prediction for predictive maintenance scheduling.

From point solutions to PHM frameworks. Existing research has made strong progress on individual PHM modules (e.g., signal-based diagnosis or learning-based prognostics). In parallel, broader "framework" efforts have emerged, particularly in digital-twin-based PHM for robot workcells and industrial robots. For example, a procedure to build a PHM-oriented digital twin for robot workcells has been presented in the context of robot performance degradation and maintenance decision-making (Kibira, Shao, & Weiss, 2021). More recently, a multi-level multi-domain industrial robot digital twin (IRDT) framework has been proposed to systematically integrate mechanical–electrical–control domains and validate the approach through pick-and-place and single-axis servo experiments (Yang et al., 2025). These studies motivate holistic PHM thinking; However, prior work provides limited end-to-end, servo-joint-focused, physics-aided PHM frameworks that explicitly address low-data

constraints, servo-induced non-stationarity, and multi-modal healthy distributions under repetitive pick-and-place operation.

Robot-joint condition monitoring and data scarcity. A practical direction for robot-joint monitoring is to utilize motor current signals as a non-invasive sensing modality because current can be collected from existing drives/controllers without installing additional sensors. Li et al. (2024) investigated industrial robot condition monitoring using different motor current signals and discussed how measurement sources affect monitoring capability in realistic settings. Electromechanical coupling modeling has also been used to link joint mechanical faults to current signatures; Xu et al. (2023) proposed a bolt-loosening detection method for an industrial robot joint based on electromechanical modeling and motor current signature analysis. Related studies also demonstrate that drivetrain faults in industrial robots (e.g., robot reducers) can be detected from embedded drive signals; for example, electrical current signature analysis has been used for RV reducer fault detection in industrial robots (Raouf, Lee, & Kim, 2022). Learning-based approaches further convert current signals into time–frequency representations and apply transfer learning to improve fault detection performance under limited fault data; Kumar et al. (2024) reported transfer-learning-based servomotor bearing fault detection in an industrial robot. Meanwhile, RUL prediction for industrial robots has advanced through deep learning architectures designed to capture multiscale temporal dependencies; More broadly, time–frequency representations combined with sequence models (e.g., wavelet-based features with LSTM) are widely used to learn degradation evolution and estimate remaining-life trajectories, motivating our CWT–LSTM regressor for continuous index prediction (Kumar et al., 2025). Gao et al. (2025) proposed a degradation-aware transformer framework that identifies the transition from healthy to degraded state and predicts RUL. Reducer-focused studies also emphasize uncertainties in degradation initiation and operating variability; Ren et al. (2024) addressed degradation onset and RUL prediction for an RV reducer by combining deep networks with support vector data description. Despite these advances, run-to-failure datasets for servo joints under diverse motion and payload conditions remain scarce, and purely data-driven approaches often struggle when degradation data are limited. This limitation has motivated physics-informed or hybrid PHM methodologies for complex systems under low-data constraints (Paquot et al., 2026).

Motivation and gap: multi-modality under trapezoidal servo operation. Pick-and-place joints typically follow repetitive trapezoidal motion profiles (acceleration–constant speed–deceleration–stop). Phase-dependent dynamics can cause healthy signals to occupy multiple clusters in feature space, undermining distance-based anomaly detection and health indicators that implicitly assume unimodal normal behavior. This is particularly problematic when PHM requires a monotonic health indicator suitable for degradation tracking and subsequent RUL interpretation. Probabilistic health indicators based on distribution modeling (e.g., GMM-based unsupervised health indices) have been explored in rotating machinery to robustly characterize degradation under distribution shift, supporting our choice of a likelihood-based indicator for multi-modal healthy behavior (Wen et al., 2024).

Proposed comprehensive physics-aided PHM framework. This paper presents a comprehensive physics-aided PHM framework for a one-degree-of-freedom servo-driven robotic joint (Figure 1). First, failure mode and effects analysis (FMEA) is used to select critical degradation mechanisms: bearing degradation (modeled as increased friction torque) and shaft misalignment (modeled as an eccentric disturbance torque). Second, to mitigate the lack of run-to-failure field data, a high-fidelity Modelica dynamic model of a motor–shaft/bearing–compliance–load drivetrain is developed to synthesize progressive degradation scenarios under trapezoidal operation. Third, we diagnose the limitation of distance-based indicators under multi-modal healthy distributions and propose a probabilistic health indicator based on a Gaussian mixture model (GMM). By fitting the GMM to healthy data and using negative log-likelihood (NLL) as the indicator, we obtain an increasing trend across the designed scenarios that supports normalized remaining useful life (Normalized-RUL) construction without requiring true failure-time labels. Finally, continuous Normalized-RUL trajectories are estimated using a continuous wavelet transform–long short-term memory (CWT–LSTM) model that learns time–frequency degradation patterns and their temporal evolution. While prior studies have addressed robot-joint condition monitoring and data-driven RUL prediction, they often treat diagnosis and prognostics as point solutions and may assume unimodal healthy behavior. In contrast, our work targets repetitive trapezoidal operation where healthy features can be phase-dependent and multi-modal, and we integrate FMEA-guided physics-based scenario design with a multi-modality-aware probabilistic HI and a normalized remaining-life target for low-label prognostics

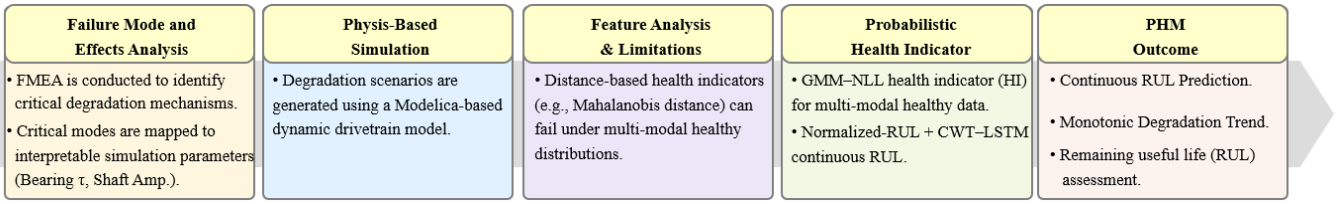

Figure 1. Overall physics-aided PHM framework for a servo-driven robotic joint.

Table 1. FMEA of servo-driven robotic joint

Primary components	Potential failure mode	Potential effects of failure	Potential factors of failure
Bearing	Degradation (friction increase)	Increased vibration Reduced repeatability/accuracy	Wear Thermal/mechanical fatigue
Shaft	Misalignment Eccentricity	Periodic vibration growth Reduced positioning accuracy	Assembly tolerance drift Deformation
Drive unit (motor/driver)	Torque margin reduction Ripple increase	Slower settling Cycle time drift	Thermal aging Parameter drift
Sensor chain	Measurement bias Noise increase	False alarms Unstable health indicator	Electrical noise Mounting looseness

The main contributions of this work are as follows:

1. An FMEA-guided selection of critical degradation mechanisms for a servo-driven joint and their mapping to physically interpretable simulation parameters (bearing friction increase and eccentric disturbance torque).

2. Physics-based degradation scenario generation using a Modelica drivetrain model to mitigate run-to-failure data scarcity under trapezoidal operation.

3. Evidence that distance-based indicators (e.g., Mahalanobis distance) can be unreliable under phase-dependent multi-modal healthy distributions.

4. A probabilistic GMM–NLL health indicator and a Normalized-RUL construction for low-label prognostics.

5. Continuous trajectory estimation using CWT–LSTM trained on the constructed Normalized-RUL target.

The remainder of this paper is organized as follows. Section 2 describes the target system and FMEA results. Section 3 presents the Modelica simulation model and degradation scenario generation. Section 4 analyzes feature distributions and limitations of distance-based health indicators. Section 5 introduces the proposed GMM–NLL health indicator and Normalized-RUL construction. Section 6 presents continuous Normalized-RUL prediction and results. Section 7 concludes the paper and outlines future work.

2. System Description and Failure Mode Analysis

2.1 Target System Description

This study targets a servo-driven robotic arm joint used in repetitive pick-and-place operations. To focus on the dominant drivetrain dynamics that govern joint health evolution, the joint is modeled as a one-degree-of-freedom (1-DOF) rotational system consisting of a motor–shaft/bearing–compliance–load drivetrain. The joint is repeatedly excited by a trapezoidal motion profile (acceleration–constant speed–deceleration–stop), which is representative of industrial pick-and-place cycles.

2.2 Failure Mode and Effects Analysis

Failure mode and effects analysis (FMEA) was performed to prioritize degradation mechanisms for a servo-driven robotic joint. As a reference baseline for servo reliability, Sung and Lee (2011) conducted a failure modes, effects, and criticality analysis (FMECA) for a servo motor by decomposing the system into primary components (bearing, stator windings, rotor, shaft, and frame) and ranking failure items using severity and frequency categories.

Their criticality results show that bearing-related failures are among the most critical items: bearing wear associated with friction-torque reduction is ranked High frequency / High severity (criticality 9), and bearing deformation is also rated high (criticality 7). Shaft-related failure items (twist and bending) are additionally listed as drivetrain-relevant modes in the same table.

Table 1 summarizes the FMEA results for the target servo-driven robotic joint and the failure modes considered in this study. In this study, the analysis is used to identify the most relevant degradation mechanisms under repetitive pick-and-place operation.

Motivated by these reliability findings and the repetitive pick-and-place operating context, this paper focuses on two critical degradation mechanisms: (i) bearing degradation,

represented as an increase in effective friction torque, and (ii) shaft misalignment, represented as an eccentric disturbance torque. These failure modes are selected because they map directly to physically interpretable parameters in the proposed simulation model and are observable through vibration-related signals used in subsequent sections.

2.3 Link to Degradation Scenario Design

The selected failure modes are directly translated into degradation scenario parameters used for physics-based simulation. Bearing degradation is implemented as a progressive increase in effective friction torque, and shaft misalignment is represented by an eccentric disturbance torque whose amplitude grows with degradation. This FMEA-to-parameter mapping enables systematic scenario generation under repetitive trapezoidal operation and supports subsequent health indicator construction and Normalized-RUL/RUL estimation.

3. Physics-Based Simulation and Degradation Scenario

3.1 Modelica-Based 1-DOF Joint Model

To mitigate the scarcity of run-to-failure datasets for industrial robot joints, we developed a physics-based simulation model using Modelica. The target joint is modeled as a 1-DOF lumped rotational drivetrain formulated as a motor–shaft/bearing–torsional-compliance–load drivetrain. The model includes (i) a motor torque source driven by a trapezoidal command, (ii) motor-side inertia, (iii) bearing friction, (iv) a torsional spring–damper element representing shaft/coupling compliance, and (v) load-side inertia. To represent shaft-related degradation, an additional disturbance torque input is superimposed on the drivetrain (Figure 2).

The model outputs joint angle $\phi(t)$, angular velocity $\omega(t)$, and angular acceleration $\alpha(t)$ via sensors. In this study, $\alpha(t)$ is used as the primary vibration-related signal for feature extraction and health monitoring because it is sensitive to friction increase and misalignment-induced excitations.

3.2 Trapezoidal Torque Parameters

Pick-and-place operation is represented by a cyclic trapezoidal command applied to the motor torque source. The trapezoidal profile parameters are set as follows: period T=0.4 s, rising time 0.05 s, plateau width 0.15 s, falling time 0.05 s, amplitude 0.25, and offset −0.125. This configuration produces a bounded repetitive excitation consistent with acceleration–constant-speed–deceleration–stop phases.

Key baseline drivetrain parameters are set to represent a realistic servo-joint dynamic response: motor inertia $J_m = 8 \times 10^{-4} kg \cdot m^2$, load inertia $J_L = 2 \times 10^{-2} kg \cdot m^2$,and a torsional spring–damper element representing shaft/coupling compliance. The spring–damper stiffness and damping parameters are selected to yield observable vibration responses under cyclic trapezoidal operation (as implemented in the Modelica spring–damper block).

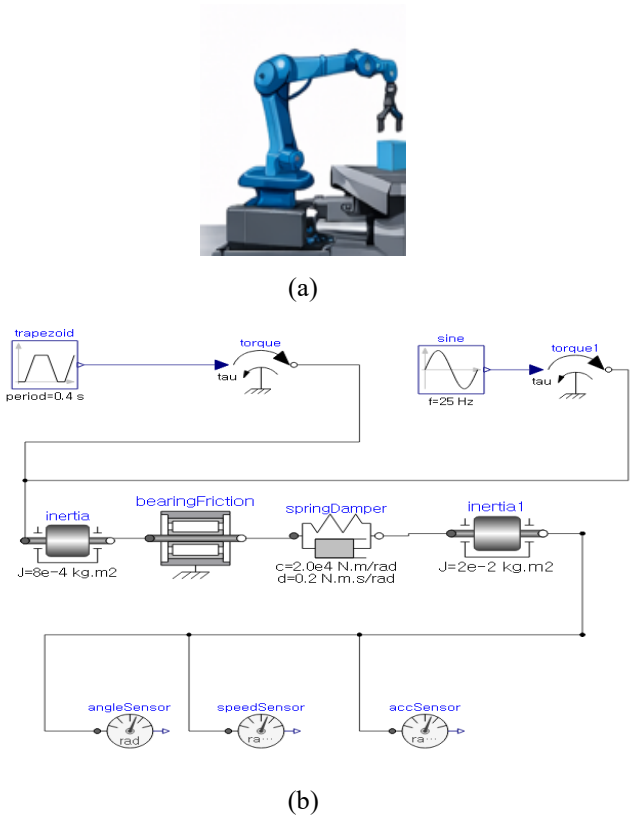

Figure 2. Target system and Modelica-based 1-DOF joint model: (a) Pick-and-place robotic arm. (b) Modelica-based 1-DOF model.

Degradation scenarios are introduced by modifying the bearing friction parameter and the eccentric disturbance torque parameters as defined in Section 3.3.

Figure 3 shows representative angular-acceleration outputs under trapezoidal operation for the healthy condition (Mode 0) and the severe degradation condition (Mode 9).

3.3 Degradation Mode Definition and Scenario

Based on the FMEA results (Section 2), we consider two critical degradation mechanisms and parameterize them for systematic scenario generation: (i) bearing degradation and (ii) shaft misalignment/eccentricity. Bearing degradation is modeled by increasing an effective bearing friction parameter (denoted as Bearing τ), while shaft misalignment is modeled by injecting an eccentric disturbance torque whose magnitude is controlled by a disturbance amplitude parameter (denoted as Shaft Amp.). Using these parameters, we define ten discrete degradation modes (Mode 0–9) to emulate progressive health deterioration under the same trapezoidal operating profile. Table 2 summarizes the degradation-mode definitions used in this study.

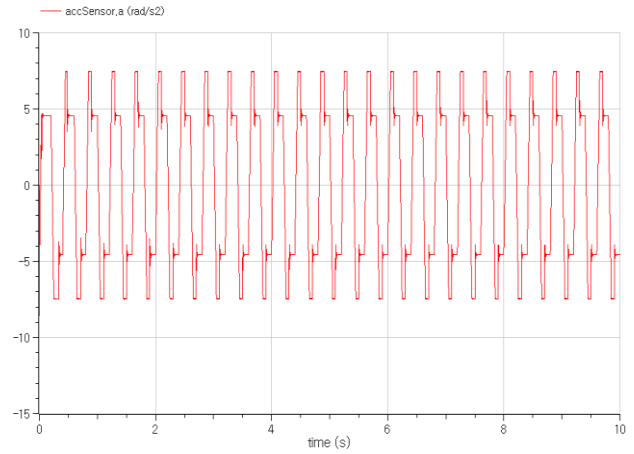

(a)

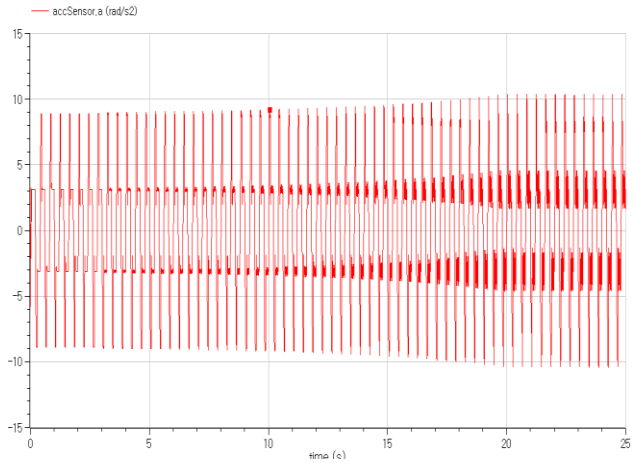

(b)

Figure 3. Angular acceleration responses under trapezoidal operation: (a) healthy (Mode 0) and (b) severe degradation (Mode 9)

Table 2. Degradation Mode

Mode & Labels	Degradation Mode	
	Bearing τ	Shaft Amp.
M0	0.030	0
M1	0.033	0
M2	0.036	0
M3	0.039	0
M4	0.042	0
M5	0.036	0.004
M6	0.039	0.006
M7	0.042	$0.002 \cdot e^{kt}$
M8	0.050	$0.002 \cdot e^{kt}$
M9	0.060	$0.002 \cdot e^{kt}$

Mode grouping and training split. Modes 0–2 represent healthy to early-stage conditions and are used as training data to learn the healthy distribution for subsequent probabilistic health-indicator modeling. Modes 3–9 represent progressive degradation up to failure-level behavior and are used for evaluation of diagnosis and prognostics. Consistent with servo PHM practice, we interpret health stages using performance-degradation criteria relative to the nominal baseline: healthy (0–5%), incipient (5–10%), degradation (10–20%), severe (20–30%), and failure ($\geq$30%). These criteria are used to guide the mode-level interpretation and thresholding strategy in later sections.

Bearing-dominant modes (M0–M4). In Modes 0–4, shaft disturbance is disabled (Shaft Amp. = 0), and degradation is introduced solely through a progressive increase in Bearing τ. This provides a controlled setting to isolate friction-related degradation effects on vibration-related signals and features.

Shaft-dominant and combined modes (M5–M9). Starting from Mode 5, shaft-related degradation is introduced by enabling the eccentric disturbance torque. In Modes 5–6, a fixed disturbance amplitude is used to represent the onset of misalignment. In Modes 7–9, the disturbance amplitude is modeled as a time-growing process to emulate progressing misalignment toward severe/failure conditions, as defined in Eq. (1):

$$\mathrm{A(t)} = A_0 \exp\{k(t - t_0)\}, \quad (1)$$

Equation (1) is used as a phenomenological scenario-generation model for the time-varying disturbance amplitude in Modes 7–9, rather than a governing equation of the drivetrain dynamics. The exponential form is adopted to represent a monotone severity progression; alternative monotone growth laws (e.g., linear or piecewise growth) can be substituted without changing the proposed framework.

where A_0 denotes the initial micro-imbalance level, k is the growth rate, and t_0 is the time offset. In our implementation, $A_0 = 0.002$, k=0.161, and $t_0 = 3$, such that the disturbance component increases exponentially as time elapses within a cycle, resulting in amplified vibration signatures under advanced misalignment conditions. The bearing friction parameter is set according to the mode definition to represent either continued bearing degradation or combined degradation, depending on the target scenario.

Dataset construction. For each mode, multiple operation cycles are simulated under identical trapezoidal excitation while varying only the degradation parameters (Bearing τ, Shaft Amp., and the time-growth parameters if applicable). The model outputs joint angle $\phi(t)$, angular velocity $\omega(t)$, and angular acceleration $\alpha(t)$. These time-series signals are later segmented into windows for feature extraction (Section 4), used to train a probabilistic health indicator from healthy modes (Section 5), and used to train and evaluate continuous

Normalized remaining useful life prediction models (Section 6).

4. Feature Engineering and Limitations of Distance-Based Health Indicators

Angular acceleration $\alpha(t)$ is used as the primary observation for health monitoring because drivetrain degradations (bearing friction increase and shaft misalignment) are more sensitively reflected in vibration-related responses than in closed-loop position/velocity signals. The signal is segmented into fixed windows under repetitive trapezoidal operation, and each window is represented by a compact time-domain feature vector: mean, RMS, standard deviation, variance, peak-to-peak, maximum, minimum, and crest factor.

Under trapezoidal motion, phase-dependent dynamics (acceleration, constant speed, deceleration, and dwell) naturally produce multi-modal feature distributions even in healthy conditions. PCA visualization confirms that healthy samples can form multiple clusters rather than a single unimodal cloud (Figure 4). This violates the implicit assumption of many distance-based health indicators.

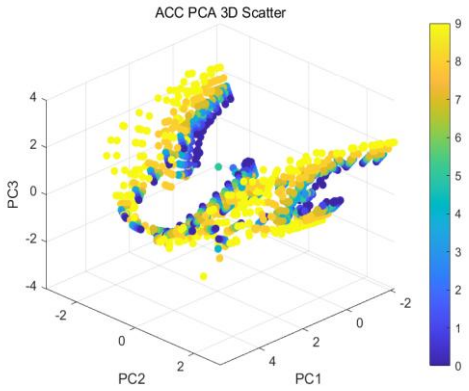

Figure 4. PCA scatter plot showing multi-modal clustering of acceleration-based features under trapezoidal servo operation.

Mahalanobis-distance-based indicators approximate healthy behavior with a single mean and covariance, which can become unreliable under multi-modality (Figure 5): (i) healthy samples from different phases may be falsely flagged as abnormal, (ii) the fitted covariance may become overly broad and overlap with degraded samples, and (iii) the resulting indicator may not increase monotonically with degradation. These observations motivate a probabilistic health indicator that explicitly models healthy multi-modality, which is addressed in Section 5 using a Gaussian mixture model and negative log-likelihood.

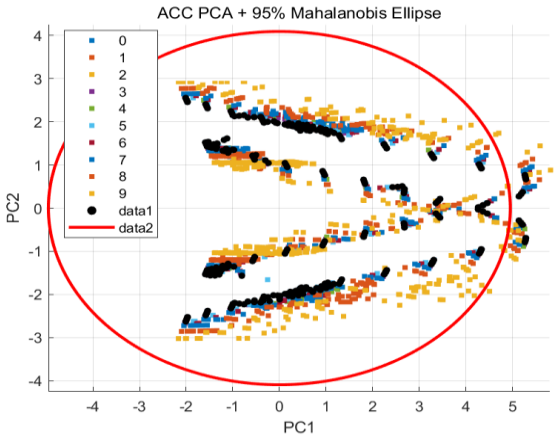

Figure 5. Limitations of Mahalanobis-distance modeling under multi-modal healthy distributions.

Black points (data1) are healthy samples (Modes 0–2), and the red ellipse (data2) is the 95% Mahalanobis ellipse fitted to the healthy set.

5. Probabilistic Health Indicator and Normalized-RUL Construction

To handle the multi-modal distribution of healthy features under trapezoidal servo operation, we model healthy feature vectors $\mathbf{x} \in \mathbb{R}^d$ using a Gaussian mixture model (GMM) as defined in Eq. (2):

$$\mathrm{p(x)} = \sum_{k=1}^{K} \pi_k \mathcal{N}(\mathrm{x}; \mu_k, \sum_k), \qquad (2)$$

where π_k are mixture weights and $(\mu_k, \sum_k)$ are component parameters. The GMM is fitted using healthy data (Mode 0–2) via maximum likelihood (e.g., EM algorithm). A probabilistic health indicator (HI) is then defined as the negative log-likelihood (NLL) under the learned healthy distribution, as given in Eq. (3):

$$\mathrm{HI(t)} = -logp\big(x(t)\big). \qquad (3)$$

Note that GMM-based NLL is not inherently guaranteed to increase monotonically with degradation. In general, NLL may behave non-monotonically if the feature trajectory approaches another high-density region of the learned healthy mixture. More generally, NLL is not a monotone degradation metric unless the degradation path moves away from (rather than along) the learned healthy manifold in feature space. In this study, under the chosen physics-parameterized degradation scenarios, the mode-wise NLL tends to increase with degradation severity, which supports its use as a relative health indicator.

Because the GMM explicitly captures multiple healthy clusters, the HI remains robust under phase-dependent multi-modality; in our simulated scenarios, it shows an increasing trend as degradation progresses.

Figure 6 presents the mode-wise distribution of the proposed HI (GMM–NLL) from Mode 0 to Mode 9.

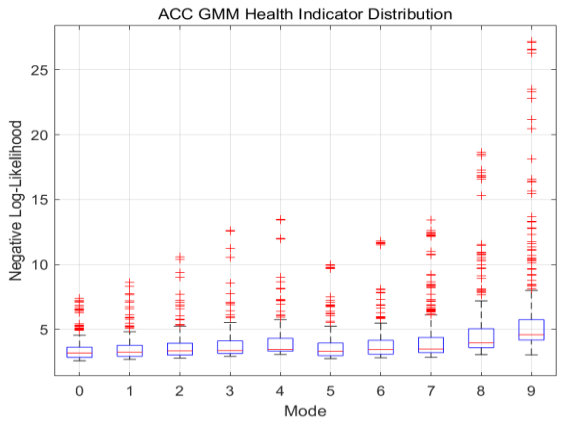

Figure 6. Distribution of the GMM–NLL health indicator across degradation modes.

To provide an RUL-like measure without ground-truth run-to-failure labels, we construct a Normalized remaining useful life (Normalized-RUL) by normalizing the HI between a healthy reference level HI_H and a failure reference level HI_F. For mode-level evaluation, we first define a representative HI for each degradation mode k as the median HI value, as defined in Eq. (4):

$$HI_k = median\{HI(t) \mid t \in \text{Mode k}\}. \quad (4)$$

We then compute Normalized-RUL for each mode k as defined in Eq. (5):

$$NormalizedRUL_k = \text{clip}\left(1 - \frac{HI_k - HI_H}{HI_F - HI_H}, 0,1\right), \quad (5)$$

Where HI_H is the median HI of healthy modes (Mode 0-2), and HI_F is defined as the 7σ threshold computed from the healthy HI distribution, as given in Eq. (6):

$$HI_F = HI_H + 7\sigma_{H,} \quad (6)$$

With σ_H denoting the standard deviation of HI over healthy modes (Mode 0–2). The selection of this 7σ threshold is grounded in both physical and statistical rationale. In reliability engineering, a 30% degradation in mechanical parameters (e.g., friction or disturbance) typically corresponds to the onset of severe structural damage and functional failure. Due to the non-linear amplification of vibration energy and the quadratic nature of log-likelihood distances, such macroscopic physical degradation forces the extracted features far outside the normal distribution. Empirically and statistically, this failure stage aligns with an extreme deviation exceeding 7σ from the healthy baseline, justifying our formulation for HI_F. Here, clip(x,0,1)=min(1,max(0,x)) confines the value to [0,1]. The resulting Normalized-RUL provides a bounded relative life index (1: healthy, 0: failure) and serves as a consistent target for subsequent continuous RUL modeling (Section 6).

In this work, 'Normalized-RUL' is a relative life index scaled between a healthy reference and a statistically defined failure reference derived from the constructed health indicator, rather than a direct estimate of time-to-failure. When time-to-failure labels become available (e.g., accelerated run-to-failure tests or field maintenance logs), this normalized index can be calibrated to a time axis by learning a mapping between the index trajectory and observed failure times. In the present study, the Normalized-RUL is used to provide a consistent prognostic target under low-label constraints and to compare degradation progression across scenarios.

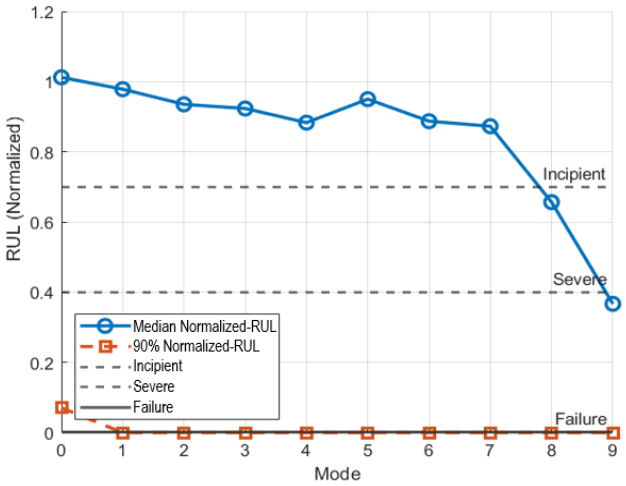

Figure 7. GMM-based Normalized-RUL across degradation modes.

6. Continuous Normalized-RUL Prediction Using CWT–LSTM

In this work, the CWT–LSTM model predicts the constructed Normalized-RUL target rather than an externally defined time-to-failure label.

To obtain a sample-level prognostic trajectory beyond mode-level Normalized-RUL (Section 5), we estimate continuous Normalized remaining useful life (Normalized-RUL) from the angular acceleration signal $\alpha(t)$ using a time–frequency deep learning approach. Each windowed segment of $\alpha(t)$ is transformed into a time–frequency representation via the continuous wavelet transform (CWT), producing a scalogram that captures degradation-sensitive spectral patterns under non-stationary trapezoidal operation. The resulting scalogram sequence is then modeled with a long short-term memory (LSTM) network to learn temporal degradation evolution and to output continuous Normalized-RUL predictions (Figure 8).

Here, the CWT–LSTM does not predict an externally defined time-to-failure quantity. Instead, it learns a regression mapping from CWT-based time–frequency patterns to the constructed Normalized-RUL target defined in Section 5, providing a continuous window-level trajectory consistent with the mode-level index.

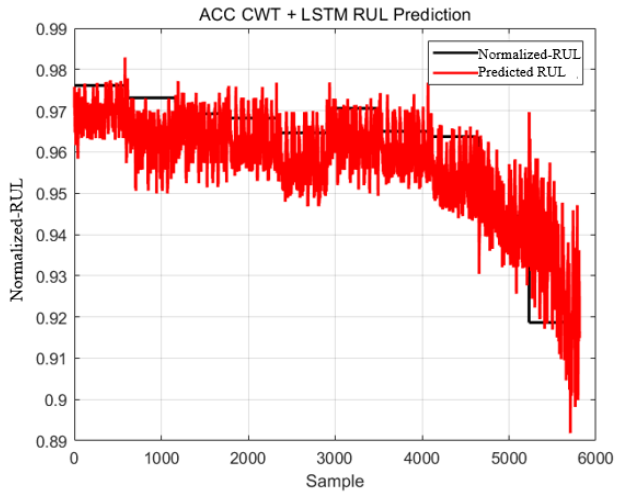

Figure 8. CWT–LSTM regression for continuous Normalized-RUL trajectory estimation.

The continuous RUL target is defined consistently with the Normalized-RUL scale (1: healthy, 0: failure) derived in Section 5 (Figure 7), enabling direct interpretation of the predicted trajectory for maintenance planning. The model is trained and evaluated on the simulated degradation scenarios (Modes 0–9, Section 3), and the Predicted RUL decreases as degradation severity increases; under the most severe simulated condition, the remaining life is reduced to approximately 40% of the nominal life.

7. Conclusion

This paper proposed a comprehensive physics-aided prognostics and health management (PHM) framework for a 1-DOF servo-driven pick-and-place robotic joint. Critical failure modes were selected via FMEA—bearing degradation and shaft misalignment—and a Modelica-based 1-DOF lumped rotational model was developed to generate progressive degradation scenarios under trapezoidal servo operation. We showed that healthy data can be multi-modal due to phase-dependent operation, which limits conventional distance-based health indicators. To address this, a probabilistic health indicator was constructed using a Gaussian mixture model (GMM) and negative log-likelihood (NLL), and a Normalized-RUL index was defined by normalizing mode-level HI between a healthy reference and a 7σ failure threshold. Finally, continuous Normalized-RUL trajectories were predicted using a CWT–LSTM model, demonstrating consistent degradation trends and reduced remaining life under severe simulated conditions.

Future work includes validating the framework with experimental data from real servo-driven robot joints, refining degradation parameter identification for improved physical fidelity, and extending the approach to multi-axis systems and varying payload/trajectory conditions. In particular, we will (i) define an application-specific EOL criterion for the servo-driven joint, (ii) calibrate Normalized-RUL trajectories to time-to-failure using accelerated tests or field maintenance logs, and (iii) evaluate prognostic performance using standard RUL metrics on the calibrated target.

Acknowledgements

This study was supported by Mobility Systems Engineering Research Program of Yonsei University (Grant No. 2024-11-0419).

REFERENCES

Gao, Z., Wang, C., Wu, J., Wang, Y., Jiang, W., & Dai, T. (2025). Degradation-aware remaining useful life prediction of industrial robot via multiscale temporal memory transformer framework. Reliability Engineering & System Safety, 262, 111176. doi:10.1016/j.ress.2025.111176

Kibira, D., Shao, G., & Weiss, B. (2021). Building a digital twin for robot workcell prognostics and health management. Proceedings of the Winter Simulation Conference (WSC 2021).

Kumar, P., Raouf, I., & Kim, H. S. (2024). Transfer learning for servomotor bearing fault detection in the industrial robot. Advances in Engineering Software, 194, 103672. doi:10.1016/j.advengsoft.2024.103672

Li, D., Zou, Z., Han, H., Lin, Y., Li, B., Huang, B., Gu, F., & Ball, A. D. (2024). Industrial robot condition monitoring using different motor current signals. In A. D. Ball, H. Ouyang, J. K. Sinha, & Z. Wang (Eds.), Proceedings of the UNIfied Conference of DAMAS, IncoME and TEPEN Conferences (UNIfied 2023) (Mechanisms and Machine Science, Vol. 151, pp. 527–538). Springer, Cham. doi:10.1007/978-3-031-49413-0_39

Paquot, L., Abisset-Chavanne, E., Rey, P.-A., Da Silva, F., & Durant, M. (2026). A physics-informed AI methodology for prognostics and health management of complex systems under low data constraints. Journal of Intelligent Manufacturing. doi:10.1007/s10845-025-02741-y

Ren, G., Wang, Z., Liu, X., & Song, F. (2024). Remaining useful life prediction of industrial robot RV reducer with multiple deep networks and multicore support vector data description. Journal of Mechanical Science and Technology, 38, 4037–4051. doi:10.1007/s12206-024-0703-y

Sung, B.-J., & Lee, J.-B. (2011). Reliability improvement of machine tool changing servo motor. Journal of International Council on Electrical Engineering, 1(1), 28–32. doi:10.5370/JICEE.2011.1.1.028

Xu, K., Wu, X., Wang, D.-X., & Liu, X. (2023). Electromechanical coupling modeling and motor current signature analysis of bolt loosening of industrial robot joint. Mechanical Systems and Signal Processing, 184, 109681. doi:10.1016/j.ymssp.2022.109681

Yang, K., Liu, Y., Tuo, B., Pan, Y., Wang, X., Zhang, L., & Wang, L. (2025). A multi-level multi-domain digital twin modeling method for industrial robots. Robotics and Computer-Integrated Manufacturing, 95, 103023. doi:10.1016/j.rcim.2025.103023

Raouf, I., Lee, H., & Kim, H. S. (2022). Mechanical fault detection based on machine learning for robotic RV reducer using electrical current signature analysis: A data-driven approach. Journal of Computational Design and Engineering, 9(2), 417–433. doi:10.1093/jcde/qwac015

Kumar, A., Wang, J., Parkash, C., Sharma, V., & Tang, H. (2025). Development of a robust wavelet divergence-based framework for health monitoring and remaining useful life estimation of gearbox. Results in Engineering, 27, 106373. doi:10.1016/j.rineng.2025.106373

Wen, L., Yang, G., Hu, L., Yang, C., & Feng, K. (2024). A new unsupervised health index estimation method for bearings early fault detection based on Gaussian mixture model. Engineering Applications of Artificial Intelligence, 128, 107562. doi:10.1016/j.engappai.2023.107562

BIOGRAPHIES

Mujin Kim has worked as a mechanical engineer at LG Display since 2010. He is currently an M.S. student in Mechanical Engineering at Yonsei University, Seoul, Republic of Korea (2025–present). He is a member of the intelligent structures and integrated design (ISID) laboratory, and his research interests include physics-aided modeling and simulation, structural analysis, and optimization.

Sejun Park received his B.S. degree in Mechanical Engineering from the Yonsei University, Seoul, Korea in 2023. He is currently pursuing an Integrated M.S. and Ph.D. student in Mechanical Engineering at Yonsei University, Seoul, Korea. His research interests are in the field of model-informed and physics-guided neural networks in areas of prognostics and health management (PHM) and industrial artificial intelligence.

Heoung Jae-Chun received the B.S. and M.S. degrees in mechanical engineering from Yonsei University, Seoul, South Korea, in 1986 and 1988, respec- tively, and the Ph.D. degree in mechanical engineering from Northwestern University, Evan- ston, Illinois, USA, in 1994. From 1990 to 1994, he was a Research Assistant at the Center for Quality Engineering and Failure Prevention, Northwest- ern University. From 1994 to 1997, he was a Post-Doctoral Research Associate at Quality Engineering and Failure Prevention, Northwestern University. In 1997, he joined the School of Mechanical Engineering, Yonsei University, where he is currently a Professor. His research interests include analysis and design of composite structures.

Jongsoo Lee received B.S. and M.S. in Mechanical Engineering at Yonsei University, Seoul, Korea and the University of Minnesota, Minneapolis, MN in 1988 and 1992, respectively and Ph.D. in Mechanical Engineering at Rensselaer Polytechnic Institute, Troy, NY in 1996. After a research associate at Rensselaer Rotorcraft Technology Center, he has been a professor of Mechanical Engineering at Yonsei University since 1997. His research interests include multi-physics design optimization (MDO), reliability-based robust optimization, virtual product design and development, model-based system engineering (MBSE), prognostics and health management (PHM), and industrial artificial intelligence.